ELSEVIER

Chemical Engineering Journal 89 (2002) 143–153

Chemical Engineering Journal

www.elsevier.com/locate/cej

Kinetic model of one-part curing system with moving boundary conditions

Tatsuro Matsui

Toray Thiokol Co., Ltd., 2-3 Chigusa Kaigan Ichihara City, Chiba Prefecture 299-0196, Japan

Received 8 September 2001; accepted 21 January 2002

Abstract

A one-part curing system is generally applied to sealants, coatings and adhesives. Most of these sealants are moisture-curable. Cure speed prediction is very important when we design or handle these materials. Kinetic models are based on the moving boundary problems of mass transfer and moisture reaction. Pseudo-steady-state (PSS) models and unsteady-state (US) models are presented for a flat plate. Both models are expressed by three dimensionless parameters. Two boundary conditions and two conditions of m (the ratio of the equilibrium water concentration of the two phases on the boundary face), $m = 1$ and $m \neq 1$, were studied using the PSS and US. The US results were completely consistent with those by another numerical method. Not only the semi-infinite but also the finite distance to cure was studied. When the dimensionless curing time θ is greater than 1, PSS is in good agreement with US under all these conditions. As most of the sealants' θ values are greater than 1, the PSS model is accurate enough for the prediction. Experimental results supported these theories. The presented models apply not only to this one-part curing system, but also to similar phenomena such as the slow reaction of the oxidation of metals in air or the degradation of a polymer by oxygen and UV or γ-radiation.

Keywords: Mass transfer; Kinetics; Mathematical modeling; Moving boundary conditions; Pseudo-steady-state; Moisture curable sealant; One-part curing system

1. Introduction

Sealant, adhesives and coatings utilize two types of systems, the one-part and the two-part systems. The former does not require any mixing of base pastes and the curing pastes, while the latter requires careful mixing of these two parts. Thus, for the ease of handling, workers prefer a one-part. There are many types of one-part curing systems, such as those activated by moisture, oxygen or UV radiation. Most one-part sealants are activated by moisture in the air, enabling easy handling, rapid curing and good stability in the package. Typical one-part sealants are urethane, silicone and polysulfide sealants [1]. Sealants composed of liquid prepolymers, fillers and plasticizer cure from the surface to the interior with time after they are extruded from the package with a hand-gun. Moisture in the air easily penetrates the cured sealants and reacts with functional terminals of these prepolymers in the uncured zone. The cured sealant zone slowly moves from the surface to the interior. The prepolymer in the uncured sealant is activated by the moisture, which is absorbed from the surface, diffuses through the cured zone to the uncured zone, and is polymerized to the elastic materials. It is very important to predict the relationship between the curing time and cured depth under some circumstances, with respect to the handling and design of these materials. These kinetic models are attributed to the moving boundary problems of mass transfer and the reaction with moisture. These phenomena are similar to the combustion of coal or the oxidation of metal in the air.

The relationship between curing time and cured depth is studied on a flat plate with a certain thickness. Two models are presented. One is the pseudo-steady-state (PSS) model, which is easy to calculate, and the other is the unsteady-state (US) model.

Wen [2] studied widely the PSS solution and US solution of solid fluid reaction models. Ishida et al. [3] and Yoshida and Kunni [4] compared the PSS model with the US model for spherical particles. All these reactions occur instantaneously on the moving boundary face. Here we study not the instantaneous reaction but the slow one, and present the PSS and US models in the one-part curing system. Under these conditions, the PSS and US models are compared for a flat plate with semi-infinite and finite thickness.

Murray and Landis [5] proposed the solution of one-dimensional heat-conduction problems involving melting and freezing, using a numerical method. A one-part

E-mail address: tatsuro_matsui@thiokol.toray.co.jp (T. Matsui).

1385-8947/02/$ – see front matter
PII: S1385-8947(02)00006-2

Nomenclature

C_i	concentration of water in the cured sealant on the surface in equilibrium with the partial pressure of water in the air (kg/m^3)
C_x	concentration of water at X when $m = 1.0$ or C_{2x} when $m \neq 1.0$ (kg/m^3)
C_1	concentration of water in the cured zone (kg/m^3)
C_2	concentration of water in the uncured zone (kg/m^3)
C_{1x}	concentration of water in the cured zone at $x_1 = X$ (kg/m^3)
C_{2x}	concentration of water in the uncured zone at $x_2 = X$ (kg/m^3)
D_1	diffusion coefficient of water in the cured zone (m^2 per day)
D_2	diffusion coefficient of water in the uncured zone (m^2 per day)
erf(x)	error function of x (–)
erfc(x)	$1 - \mathrm{erf}(x)$ (–)
k	reaction rate constant (1 per day)
k'	total weight of water consumed for curing per unit volume (kg/m^3)
k_1	reaction rate constant at the first step (1 per day)
k_2	reaction rate constant at the second step (1 per day)
L	upper limit of X or x_2 (m)
m	$C_2(X)/C_1(X) = C_{2x}/C_{1x}$ (–)
N	flux of water (kg/(m^2 day))
N_1	flux of water in the cured zone (kg/(m^2 day))
N_2	flux of water in the uncured zone (kg/(m^2 day))
Q	total flux of water from 0 to cured time T for curing at any uncured face (kg/m^2)
r	D_2/D_1 (–)
R_c	rate of water consumption by the reaction (kg/(m^2 day))
RH	relative humidity (%)
S	operator of Laplace transformation
t	time (day)
T	curing time (day)
x	uncured distance $= x_2 - X$ (m)
x_1	distance from the surface in the cured zone (m)
x_2	distance from the surface in the uncured zone (m)
X	distance of the boundary face from the surface or cured depth (m)

Greek letters

ξ	dimensionless cured depth or distance $(=(X/2)\sqrt{k/D_1})$ (–)
ξ_0	dimensionless upper limit distance $(=(L/2)\sqrt{k/D_1})$ (–)
η	dimensionless distance $(=((L-X)/2)\sqrt{k/D_1})$ (–)
θ	dimensionless curing time $(=kT)$ (–)
λ	dimensionless variable $(=x_1/\sqrt{4D_1t})$ (–)

curing model is applied to this method. The results by Murray's method completely coincide with those by our US model. The experimental results are compared with those obtained from our models.

2. Model

A schematic moisture concentration profile of the sealant is shown in Fig. 1. The moisture concentration on the sealant surface is in equilibrium with that in air. Moisture transfers through the cured zone (diffusion zone), where moisture is not consumed by the reaction but simply diffuses to the uncured zone (reaction zone) where moisture disappears due to its reaction. The boundary face between the cured zone and uncured zone moves with time from the surface into the interior. On the boundary face, C_{1x} in the cured zone and C_{2x} in the uncured zone are assumed to be in equilibrium instantaneously ($m = C_{2x}/C_{1x}$). The reaction rate is assumed to be proportional to the moisture concentration in the sealant. For easy calculation, we assume that the diffusion coefficient D_2 is constant in the reaction zone and that the concentration of water on the boundary zone changes discontinuously from C_{1x} to C_{2x}.

Two moving boundary conditions (cases 1 and 2) of the PSS and US models are studied. Each models has $m = 1$ and $m \neq 1$. First, the PSS models for cases 1 and 2 are presented because of simplicity of understanding and calculation. Next, the US models for cases 1 and 2 are presented. A special value of $m = 1$ is studied for both models. In the

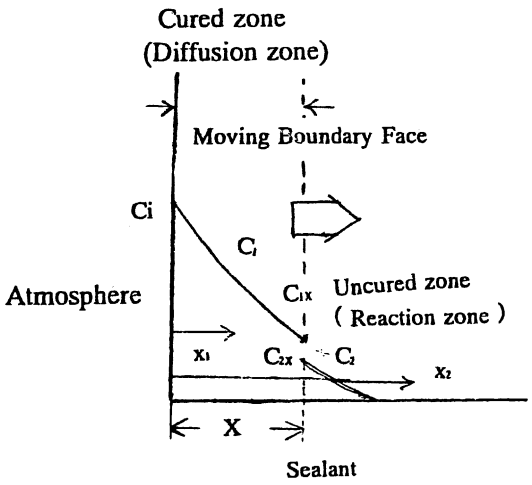

Fig. 1. Schematic moisture profile in the sealant.

next section, these models are studied by numerical calculations, and the US model is verified by another numerical method.

2.1. PSS model

In the diffusion zone and the reaction zone, the stationary state holds good. The boundary face between them moves with time. From the stationary state in Fig. 1, the flux of water in the cured zone (or diffusion zone) is expressed by

$$N_1 = \frac{D_1(C_i - C_{1x})}{X} \tag{1}$$

In the uncured zone (or reaction zone), if water consumption rate is proportional to the water concentration, Eq. (2) is described from the stationary state under semi-infinite conditions:

$$D_2 \frac{\mathrm{d}^2 C_2}{\mathrm{d}x^2} = kC_2 \tag{2}$$

at boundary conditions $x = 0, C_2 = C_x$ and $x = \infty, C_2 = 0$.From Eq. (2) and the B.C., the flux of water in the uncured zone on the boundary face is given by

$$N_2 = -D_2 \left(\frac{\mathrm{d}C_2}{\mathrm{d}x}\right)\bigg|_{x=0} = \sqrt{kD_2}C_{2x} \tag{3}$$

We assume that N_1 in Eq. (1) is equal to N_2 in Eq. (3) and, furthermore, if C_{2x} is in equilibrium with C_{1x} and defined by $C_{2x} = mC_{1x}$, then Eq. (4) is obtained:

$$N = \frac{C_i}{X/D_1 + 1/m\sqrt{kD_2}} \tag{4}$$

2.1.1. PSS model of case 1

We postulate that the velocity of the moving boundary face, or curing speed, is proportional to the transfer rate of water on the boundary face. That is, the proportional constant, k', is the water consumption for curing per unit volume:

$$N\,\mathrm{d}T = k'\,\mathrm{d}X \tag{5}$$

where T is the curing time and X the cured depth.

From Eqs. (4) and (5), N is eliminated, and we get

$$\frac{\mathrm{d}X}{\mathrm{d}T} = \left(\frac{C_i}{k'}\right)\left(\frac{1}{X/D_1 + 1/m\sqrt{kD_2}}\right) \tag{6}$$

at initial conditions $T = 0$, $X = 0$.

Eq. (6) is integrated, yielding Eq. (7) of PSS

$$T = \left(\frac{k'}{C_i}\right)\left(\frac{X^2}{2D_1} + \frac{X}{m\sqrt{kD_2}}\right) \tag{7}$$

A dimensionless parameter and variables are introduced into Eq. (7) to obtain

$$r = \frac{D_2}{D_1}, \qquad \theta = kT, \qquad \xi = \frac{x}{2}\sqrt{\frac{k}{D_1}}$$

The dimensionless equation (8) is thus obtained:

$$\theta = 2.0\left(\frac{k'}{C_i}\right)\left(\xi^2 + \frac{1}{m\sqrt{r}}\xi\right) \tag{8}$$

For $m = 1$ in Eq. (8), Eq. (9) is obtained:

$$\theta = 2.0\left(\frac{k'}{C_i}\right)\left(\xi^2 + \frac{1}{\sqrt{r}}\xi\right) \tag{9}$$

2.1.2. PSS model of case 2

For the condition of case 1, Eq. (5) seems to be intuitive. A more theoretical boundary condition has to be considered. We postulate that after the total flux from $t = 0$ to T at any uncured point or face has reached a specified value, its point or face changes from the uncured region to the cured region and its specified value is constant wherever it is located. Total absorption water on this face is consumed by curing reaction and its diffusion into the uncured zone. Its value is constant to be cured at any point. This assumption leads to the following equation (Appendix A)

$$C_{2x} + k' = N_2|_{x_2=X}\frac{\mathrm{d}T}{\mathrm{d}X} \tag{10}$$

From Eqs. (1) and (3) and $C_{2x} = mC_{1x}$, C_x $(=C_{2x})$ is obtained and given as

$$C_x = \frac{C_i}{1/m + (\sqrt{kD_2}/D_1)X} \tag{11}$$

From Eqs. (3), (10) and (11), Eq. (12) is obtained:

$$\left(\frac{C_i/\sqrt{kD_2}}{1/m\sqrt{kD_2} + X/D_1} + k'\right)\mathrm{d}X = \frac{C_i}{X/D_1 + 1/m\sqrt{kD_2}}\,\mathrm{d}T \tag{12}$$

at initial conditions $T = 0$, $X = 0$.

Integration of Eq. (12) yields the following equation

$$T = \left(\frac{1 + k'/mC_i}{\sqrt{kD_2}}\right)X + \left(\frac{k'/C_i}{2D_1}\right)X^2 \tag{13}$$

Dimensionless equation of Eq. (13) is given by Eq. (14)

$$\theta = 2\left(\frac{k'}{C_i}\right)\left\{\xi^2 + \frac{1}{m\sqrt{r}}\left(1 + \frac{C_i}{k'}\right)\xi\right\} \tag{14}$$

For $m = 1$, Eq. (15) is obtained:

$$\theta = 2\left(\frac{k'}{C_i}\right)\left\{\xi^2 + \frac{1}{\sqrt{r}}\left(1 + \frac{C_i}{k'}\right)\xi\right\} \tag{15}$$

2.2. US model

In the cured zone, there are no reaction as shown in Fig. 1. In the cured zone

$$\frac{\partial C_1}{\partial t} = D_1\frac{\partial^2 C_1}{\partial X_1^2} \tag{16}$$

$$\text{B.C.} \quad \begin{array}{ll} x_1 = 0, & C_1 = C_i \\ x_1 = X, t = T, & C_1 = C_{1x} \end{array}$$

Wen [1] analyzed an equation similar to Eq. (16). From Eq. (16), Eq. (17) is obtained by the introduction of dimensionless variable $\lambda = x_1/\sqrt{4D_1t}$:

$$C_1(x_1) = C_i - \frac{(C_i - C_{1x})\,\mathrm{erf}(x_1/2\sqrt{D_1t})}{\mathrm{erf}(X/2\sqrt{D_1T})} \tag{17}$$

In the uncured zone, the reaction and the diffusion of water occur simultaneously, as shown in Fig. 1. If the reaction rate is assumed to be the first-order of water concentration, Eq. (18) is expressed. Examples of the reaction scheme will be described in Section 6.

In the uncured zone

$$\frac{\partial C_2}{\partial t} = D_2\frac{\partial^2 C_2}{\partial x_2^2} - kC_2 \tag{18}$$

$$\text{B.C.} \quad \begin{array}{ll} x_2 = \infty, & C_2(x_2) = 0 \\ x_2 = X, t = T, & C_2 = C_{2x} \end{array}$$

Laplace transformation of Eq. (18) is given by Eq. (19)

$$\frac{\mathrm{d}^2 C_2(S)}{\mathrm{d}x_2^2} = \left(\frac{S}{D_2} + \frac{k}{D_2}\right) C_2(S) \tag{19}$$

$$\text{B.C.} \quad x_2 = \infty, C_2(S) = 0, \qquad x_2 = X, C_2(S) = \frac{C_{2x}}{S} \tag{20}$$

C_{2x} is a function of only $X(T)$ or an independent variable, i.e., curing time T, and does not depend on t. The relationship between X and T is defined by Eq. (5) in case 1 or by Eq. (10) in case 2.

From Eqs. (19) and (20), Eq. (21) is obtained:

$$C_2(S) = \frac{C_{2X}}{S}\exp\left(-\frac{x_2 - X}{\sqrt{D_2}}\sqrt{S+k}\right) \tag{21}$$

The inverse Laplace transformation of Eq. (21) [6] is described by Eq. (22):

$$\begin{aligned} C_2(x_2) = \frac{C_{2x}}{2}\Bigg[&\exp\left\{-\sqrt{\frac{k}{D_2}}(x_2 - X)\right\} \\ &\times \mathrm{erfc}\left(\frac{x_2 - X}{2\sqrt{D_2t}} - \sqrt{kt}\right) + \exp\left\{\sqrt{\frac{k}{D_2}}(x_2 - X)\right\} \\ &\times \mathrm{erfc}\left(\frac{x_2 - X}{2\sqrt{D_2t}} + \sqrt{kt}\right)\Bigg] \end{aligned} \tag{22}$$

Danckwerts' moving boundary condition [7,8] of two phases is expressed by Eq. (23):

$$\begin{aligned} D_1\left(\frac{\partial C_1}{\partial x_1}\right)_{x_1=X} - D_2\left(\frac{\partial C_2}{\partial x_2}\right)_{x_2=X} \\ + C_{2x}\left(\frac{1}{m} - 1\right)\frac{\mathrm{d}X}{\mathrm{d}T} = 0 \end{aligned} \tag{23}$$

If we assume that $m = C_{2x}/C_{1x} = 1.0$, then

$$D_1\left(\frac{\partial C_1}{\partial x_1}\right)_{x_1=X} = D_2\left(\frac{\partial C_2}{\partial x_2}\right)_{x_2=X} \tag{24}$$

From Eq. (23), Eq. (25) is obtained:

$$\frac{\mathrm{d}X}{\mathrm{d}T} = \frac{D_2(\partial C_2/\partial x_2)_{x_2=X} - D_1(\partial C_1/\partial x_1)_{x_2=X}}{C_x(1/m - 1)} \tag{25}$$

From Eq. (17), Eq. (26) is obtained:

$$\left.\frac{\partial C_1}{\partial x_1}\right|_{x_1=X} = \frac{-(C_i - C_{1x})\exp\{-(X^2/4D_1T)\}}{\sqrt{\pi D_1T}\,\mathrm{erf}(X/2\sqrt{D_1T})} \tag{26}$$

From Eq. (22), Eq. (27) is obtained:

$$\left.\frac{\partial C_2}{\partial x_2}\right|_{x_2=X} = C_{2x}\left\{\frac{-\exp(-kT)}{\sqrt{\pi D_2T}} - \sqrt{\frac{k}{D_2}}\,\mathrm{erf}\sqrt{kT}\right\} \tag{27}$$

2.2.1. US model of case 1

We postulate that the boundary face rate or the curing speed is proportional to the water transfer rate on the boundary face under the following condition, as explained in Section 2.1.1:

$$N(x_2 = X)\,\mathrm{d}T = k'\,\mathrm{d}X \tag{5a}$$

From Eqs. (5a) and (25)–(27), the following quadratic equation in C_x is obtained:

$$\begin{aligned} &\left\{\frac{\exp(-kT)}{\sqrt{\pi kT}} + \mathrm{erf}\sqrt{kT}\right\}\left(\frac{1}{k'}\right)C_x^2 + \frac{1}{1/m - 1} \\ &\times\left\{\frac{\exp(-X^2)}{m\sqrt{r}\sqrt{\pi kT}\,\mathrm{erf}(X/2\sqrt{D_1T})} + \frac{\exp(-kT)}{\sqrt{\pi kT}} + \mathrm{erf}\sqrt{kT}\right\} \\ &\times C_x - \frac{C_i\exp(-X^2/4D_1T)}{(1/m - 1)\sqrt{r}\sqrt{\pi kT}\,\mathrm{erf}(X/2\sqrt{D_1T})} = 0 \end{aligned} \tag{28}$$

The dimensionless equation of Eq. (28) is given by Eq. (29):

$$\begin{aligned} &\left\{\frac{\exp(-\theta)}{\sqrt{\pi\theta}} + \mathrm{erf}\sqrt{\theta}\right\}\left(\frac{1}{k'}\right)C_x^2 + \left[\frac{1}{1/m - 1}\right. \\ &\left.\times\left\{\frac{\exp(-\xi^2/\theta)}{m\sqrt{r}\sqrt{\pi\theta}\,\mathrm{erf}(\xi/\sqrt{\theta})} + \frac{\exp(-\theta)}{\sqrt{\pi\theta}} + \mathrm{erf}\sqrt{\theta}\right\}\right]C_x \\ &- \frac{C_i\exp(-\xi^2/\theta)}{(1/m - 1)\sqrt{r}\sqrt{\pi\theta}\,\mathrm{erf}(\xi/\sqrt{\theta})} = 0 \end{aligned} \tag{29}$$

For $m = 1$, C_x is expressed by Eqs. (24), (26) and (27) and $C_{2x} = C_{1x}$ $(=C_x)$:

$$\begin{aligned} C_x = &\frac{C_i\exp(-X^2/4D_1T)}{\exp\{-(X^2/4D_1T)\} + \sqrt{D_2/D_1}} \\ &\{\sqrt{k}\,\mathrm{erf}\sqrt{kT} + (1/\sqrt{\pi T})\exp(-kT)\} \\ &\sqrt{\pi T}\,\mathrm{erf}(X/2\sqrt{D_1T}) \end{aligned} \tag{30}$$

Eq. (30) is converted to the dimensionless equation (31) by the introduction of dimensionless parameters.

$$\frac{C_x}{C_i} = \frac{\exp(-\xi^2/\theta)}{\exp(-\xi^2/\theta) + \sqrt{r}\{\sqrt{\pi\theta}\,\mathrm{erf}\sqrt{\theta} + \exp(-\theta)\}} \times \mathrm{erf}(\xi/\sqrt{\theta}) \quad (31)$$

From Eqs. (5a) and (27), Eq. (32) is obtained:

$$\frac{\mathrm{d}X}{\mathrm{d}T} = \frac{N}{k'} = \left(\frac{D_2 C_x}{k'}\right)\left\{\frac{\exp(-kT)}{\sqrt{\pi D_2 T}} + \sqrt{\frac{k}{D_2}}\,\mathrm{erf}\sqrt{kT}\right\} \quad (32)$$

When Eq. (31) is substituted into Eq. (32), dimensionless equation (33) is obtained:

$$\frac{\mathrm{d}\xi}{\mathrm{d}\theta} = \left(\frac{\sqrt{r}}{2\sqrt{k'/C_i}}\right)\frac{\exp(-\xi^2/\theta)\{\exp(-\theta)/\sqrt{\pi\theta} + \mathrm{erf}\sqrt{\theta}\}}{\{\exp(-\xi^2/\theta) + \sqrt{r}(\sqrt{\pi\theta} + \mathrm{erf}\sqrt{\theta} + \exp(-\theta)\,\mathrm{erf}(\xi/\sqrt{\theta})\}} \quad (33)$$

The initial condition of Eq. (33) at $\theta = 0$ is $\xi = 0$.

Eq. (33) gives the curing speed of the US model for case 1 and $m = 1$.

2.2.2. US model of case 2

In this section, the US model of case 2 is studied.

From Eqs. (10) and (25)–(27), the quadratic equation in C_x is determined as follows:

$$\left[\frac{1}{1/m-1}\left\{\frac{\exp(-\theta)}{\sqrt{\pi\theta}} + \mathrm{erf}\sqrt{\theta} + \frac{\exp(-\xi^2/\theta)}{m\sqrt{r}\sqrt{\pi\theta}\,\mathrm{erf}(\xi/\sqrt{\theta})}\right\} + \frac{\exp(-\theta)}{\sqrt{\pi\theta}} + \mathrm{erf}\sqrt{\theta}\right] C_x^2 + \left[\frac{k'}{1/m-1} \times \left\{\frac{\exp(-\xi^2/\theta)}{m\sqrt{r}\sqrt{\pi\theta}\,\mathrm{erf}(\xi/\sqrt{\theta})} + \frac{\exp(-\theta)}{\sqrt{\pi\theta}} + \mathrm{erf}\sqrt{\theta}\right\} - \frac{C_i \exp(-\xi^2/\theta)}{(1/m-1)\sqrt{r}\sqrt{\pi\theta}\,\mathrm{erf}(\xi/\sqrt{\theta})}\right] C_x - \frac{C_i k' \exp(-\xi^2/\theta)}{(1/m-1)\sqrt{r}\sqrt{\pi\theta}\,\mathrm{erf}(\xi/\sqrt{\theta})} = 0 \quad (34)$$

For $m = 1$, $\mathrm{d}X/\mathrm{d}T$ is expressed by Eqs. (10) and (27) and $C_{2x} = C_{1x}$ ($=C_x$).

$$\frac{\mathrm{d}X}{\mathrm{d}T} = \left(\frac{D_2}{1 + k'/C_x}\right)\left(\frac{\exp(-kT)}{\sqrt{\pi D_2 T}} + \sqrt{\frac{k}{D_2}}\,\mathrm{erf}\sqrt{kT}\right) \quad (35)$$

When Eq. (31) is substituted in Eq. (35), dimensionless equation (36) is obtained:

$$\frac{\mathrm{d}\xi}{\mathrm{d}\theta} = \frac{\sqrt{r}}{2}\left\{\frac{\exp(-\theta)}{\sqrt{\pi\theta}} + \mathrm{erf}\sqrt{\theta}\right\}\left(\frac{1}{1 + k'/C_x}\right) = \frac{\sqrt{r}}{2}\frac{\{\exp(-\theta)/\sqrt{\pi\theta} + \mathrm{erf}\sqrt{\theta}\}}{[1 + (k'/C_i)\{1 + \sqrt{r}\{\sqrt{\pi\theta}\,\mathrm{erf}\sqrt{\theta} + \exp(-\theta)\}\,\mathrm{erf}(\xi/\sqrt{\theta})/\exp(-\xi^2/\theta)\}]} \quad (36)$$

The initial conditions of Eq. (36) at $\theta = 0$ is $\xi = 0$. Eq. (36) gives the curing speed of the US model for case 2 and $m = 1$.

3. Numerical calculations

According to the above models, one-part curing systems can be examined using numerical calculations.

3.1. Comparison between PSS and US models for case 1 and the effect of parameters

First, the relationship between the cured depth and the curing time is calculated using Eq. (9) in the PSS model and using Eq. (33) in the US model for $m = 1$.

Fig. 2 shows ξ vs. θ of the PSS and US models. The values of ξ in both models are in good agreement when θ is greater than 1.

3.1.1. Effect of parameter k'/C_i

The effect of k'/C_i is shown in Fig. 3. If k'/C_i is increased, $\mathrm{d}\xi/\mathrm{d}\theta$ or the curing speed is decreased.

3.1.2. Effect of parameter r

The effect of r is shown in Fig. 4. If r is increased, $\mathrm{d}\xi/\mathrm{d}\theta$ or the curing speed is only slightly increased when θ and r are less than 1. This means that D_2 slightly affects the curing speed when θ is less than 1.

3.1.3. Effect of parameter m

Fig. 5 compares of the PSS model's results using Eq. (8) and the US model's results using Eqs. (29) and (32). Both models are also in good agreement when θ is greater than 1. The effect of m in case 1 is shown in Fig. 6. The parameter m affects ξ and θ little but has a slight effect when m is less than 1 and θ is less than 1.

3.2. Comparison between PSS and US models in case 2 and effect of parameters

First, the relationship between the cured depth and the curing time is calculated using Eq. (15) for the PSS model and using Eq. (36) for the US model for $m = 1$. Fig. 7 shows ξ vs. θ for the PSS and US models. The values of ξ in both models are in good agreement when θ is greater than 1. This relationship, shown in Fig. 7, is similar to that for case 1 shown in Fig. 2.

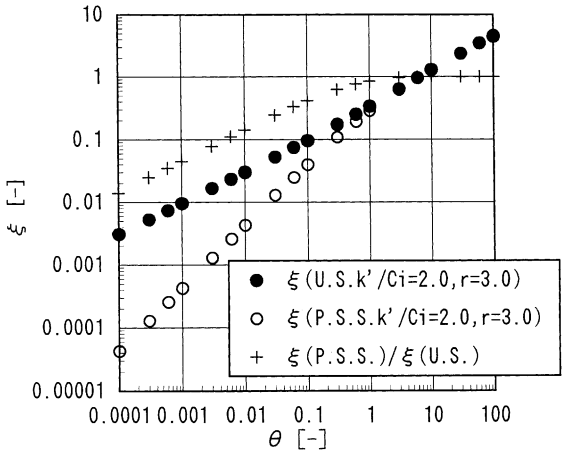

Fig. 2. Relationship between θ and ξ (case 1 and $m = 1$).

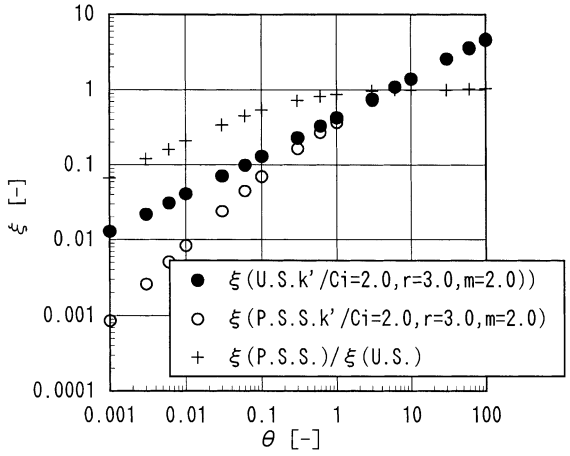

Fig. 5. Relationship between θ and ξ (case 1 and $m = 2$).

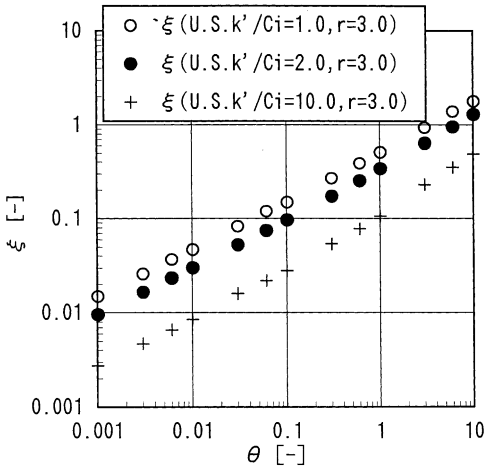

Fig. 3. Influence of k'/C_i (case 1 and $m = 1$).

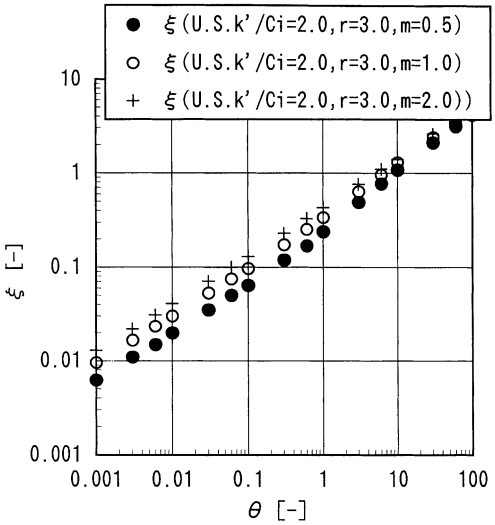

Fig. 6. Influence of m (case 1).

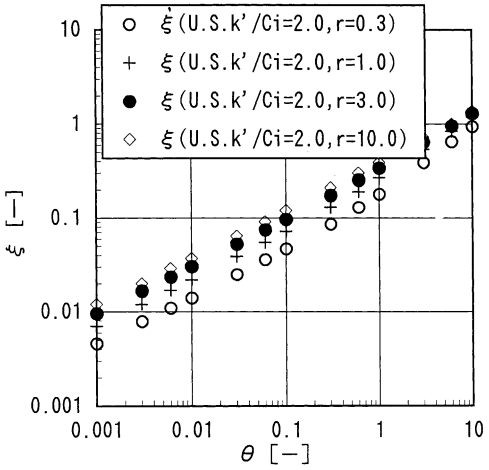

Fig. 4. Influence of r (case 1 and $m = 1$).

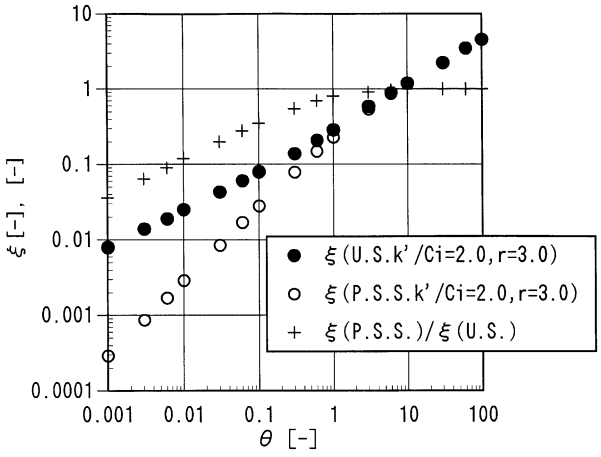

Fig. 7. Comparison of PSS and US (case 2 and $m = 1$).

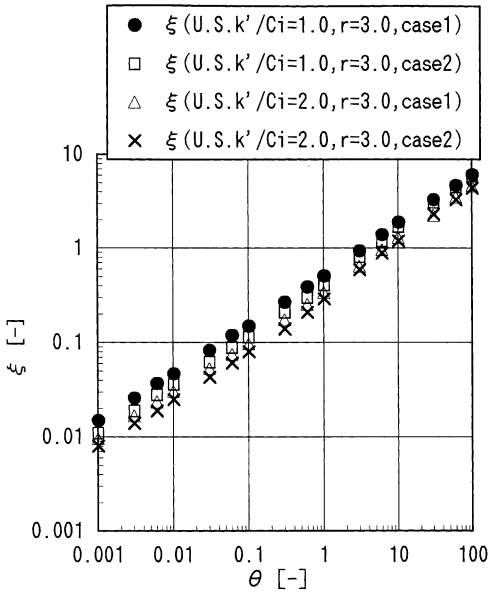

Fig. 8. Comparison of cases 1 and 2 ($m = 1$).

3.2.1. Comparison of cases 1 and 2

Fig. 8 compares the US model in cases 1 and 2 for $m = 1$. The curing speed for case 1 is slightly faster than that for case 2 under the same conditions. If $k' \geq C_i \gg C_{2x}$ as shown in Fig. 1, the boundary condition for case 1 by Eq. (5a) is almost the same as that for case 2 by Eq. (10), and the two results are almost the same especially when θ is greater than 1.

3.2.2. Effect of parameter m

From Eqs. (10) and (27), the US model of Eq. (37) or dimensionless equation (38) is obtained:

$$\frac{dX}{dT} = \frac{N}{k' + C_x} = \left\{\frac{D_2 C_x}{k' + C_x}\right\} \times \left\{\frac{\exp(-kT)}{\sqrt{\pi D_2 T}} + \sqrt{\frac{k}{D_2}}\,\mathrm{erf}\sqrt{kT}\right\} \quad (37)$$

$$\frac{d\xi}{d\theta} = \frac{\sqrt{r}}{2}\left(\frac{1}{1 + k'/C_x}\right)\left\{\frac{\exp(-\theta)}{\sqrt{\pi\theta}} + \mathrm{erf}\sqrt{\theta}\right\} \quad (38)$$

The initial condition of Eq. (38) at $\theta = 0$ is $\xi = 0$.

The effect of m in case 2 by Eqs. (34) and (38) is shown in Fig. 9

. The effect of m on θ and ξ is small, but it has a slight effect when m is less than 1 and θ is less than 1. This result is the same as that in case 1, as shown in Fig. 6.

3.3. Comparison between US model and Murray's method

In order to evaluate these US models, another numerical solution by Murray's method [5] was applied to one-part curing conditions (case 1 and $m = 1$). From Eqs. (5a), (16), (18) and (24), the algorithm of Murray's method (fixed space network) was programmed, in which the partial differential equation was converted to the difference equation. The results of this method were compared with those of the US model equation (33) (case 1 and $m = 1$). Both results are shown in Fig. 10. They are completely coincident. Thus, the US models are mathematically adequate.

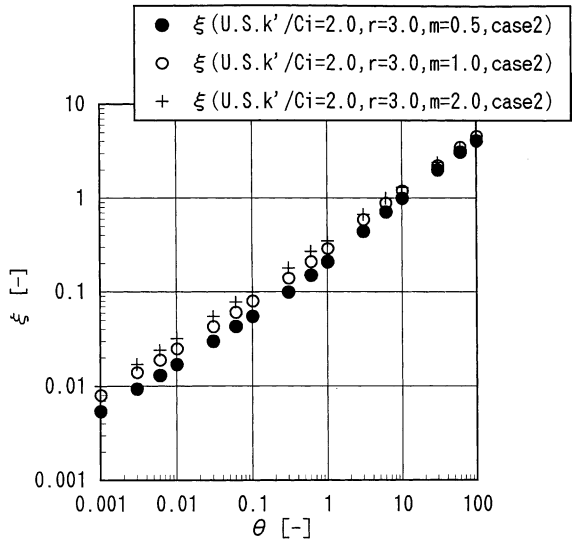

Fig. 9. Influence of m (case 2).

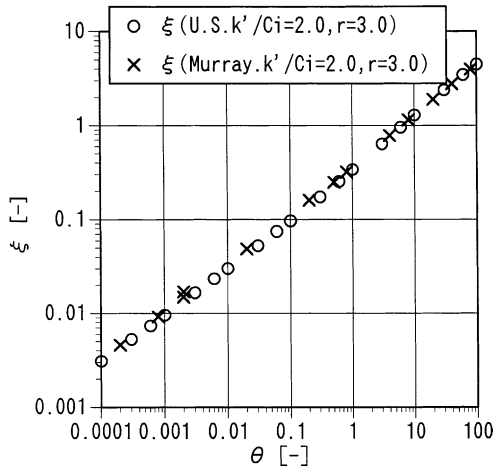

Fig. 10. Comparison between US model and Murray's method ($k'/C_i = 2.0$, $r = 3.0$, $m = 1$ and case 1).

4. Illustration of the computed results

The numerical results of the PSS and US models were compared. If θ is greater than 1, the results of the PSS and US models are in good agreement. Two boundary condition models of $m \neq 1$ and $m = 1$ were presented. All these four cases had similar results. The influence of r and m on the US models were studied. The m and r values of less than 1 had a much greater influence than those with m and r

greater than 1 for cases 1 and 2. These results show that the rate-determining step does not depend on the conditions in the uncured zone but on the conditions in the cured zone.

The slope of ξ and θ from the US model results are nearly 1/2 as plotted on log–log paper (Figs. 2–9).

$$\xi = \left(\frac{X}{2}\right)\sqrt{\frac{k}{D_1}} = K\theta^{1/2} = K(kT)^{1/2},$$

$$X = 2K\sqrt{\frac{D_1}{k}}(kT)^{1/2}, \qquad X \propto 2K(T)^{1/2}\sqrt{D_1}$$

This means that X is proportional to the square root of T and D_1 and does not depend on the reaction rate constant k. When θ is greater than 1, the slopes of $\log\xi$ and $\log\theta$ from the US and PSS models are 1/2. However, when θ is less than 1, the slope from the PSS models is almost equal to 1, while the slope from the US models remains at almost 1/2 as θ decreases. Two boundary conditions were studied. Case 2 is more accurate than case 1 theoretically and phenomenally. However, the two results are almost the same according to Fig. 8. Thus, it is accurate enough to consider mathematically case 1.

5. Comparison between experiments and models

At constant temperature and humidity, the cured depth of the sealant was measured at specified times T. Urethane sealant was measured at 20 °C and RH 100%. Polysulfide sealant was measured at 20 °C and RH 100 and 30%. Silicone sealant was measured at 20 °C and RH 30%. We assumed that C_i is proportional to RH.

C_iD_1 was measured by moisture permeability through the cured sealant according to the JIS Z 0208. Samples of cured sealant were crushed and kept at constant temperature and humidity for enough time. These samples were titrated by Karl–Fisher's method, and C_i was observed and D_1 was separated and calculated from the moisture permeability. k' and k were measured by supposition between actual cured depth and curing time. These parameters are shown in Table 1 [9]. Experimental data for urethane, silicone and polysulfide sealants [9] were compared with the PSS model equation (9) of $m = 1$, $r = 1$ and case 1. The PSS models were accurate enough because θ is more than 1 and it is not necessary to consider the US models. Furthermore, Eq. (9) of case 1 is accurate enough compared with Eq. (15) of case 2. We considered that r and m are 1 in this case. Fig. 11 compares experiments and models. The results show good coincidence.

Table 1
Parameters of sealants at 20 °C

	k'	$D_1 = D_2$	C_i	k
Urethane	12	0.73×10^{-5}	13.5 (RH = 100%)	1.1
Polysulfide	5.6	1.55×10^{-5}	4.6 (RH = 100%)	5.4
			1.4 (RH = 30%)	
Silicone	16	13.6×10^{-5}	0.33 (RH = 30%)	643

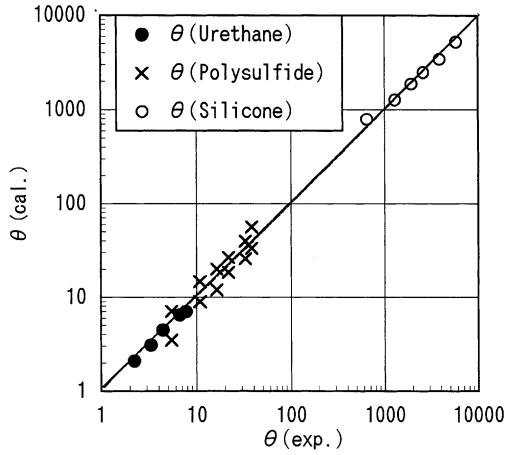

Fig. 11. Relationship between experimental θ and calculated θ.

6. Discussion

Many researchers have tried to solve the moving boundary problems of two phases where reactions occur instantaneously on the boundary face. This work solves the moving boundary problems of two phases where in one phase diffusion occurs and in the other phase a slow reaction and diffusion occurs. One good example is a moisture-curable one-part sealant. One phase is the cured zone (diffusion region) or the elastic solid phase, and the other phase is the uncured zone (reaction region) or viscous fluid zone. There are three types of representative moisture-curable one-part elastic sealants: silicone, urethane and polysulfide sealants. Most contain moisture-sensitive prepolymers, i.e., protective functional groups that are bonded to the terminals of their prepolymers and that first react with the moisture absorbed from the atmosphere and are converted to active terminals. These active terminals then combine with each other and are polymerized to form the elastic rubber.

protective functional group of prepolymer + H_2O
$\xrightarrow{k_1}$ active terminals of prepolymer + byproducts (39)

active terminals (+catalyst + curing agents)
$\xrightarrow{k_2}$ polymerization to solid (elastic rubber)

In the other type, when the latent catalyst is converted to the active catalyst by moisture absorbed from the atmosphere, the prepolymer in the sealant is polymerized by this active catalyst.

latent catalyst + H_2O
$\xrightarrow{k_1}$ active catalyst prepolymer
+active catalyst (+curing agents)
$\xrightarrow{k_2}$ polymerization to solid (elastic rubber) (40)

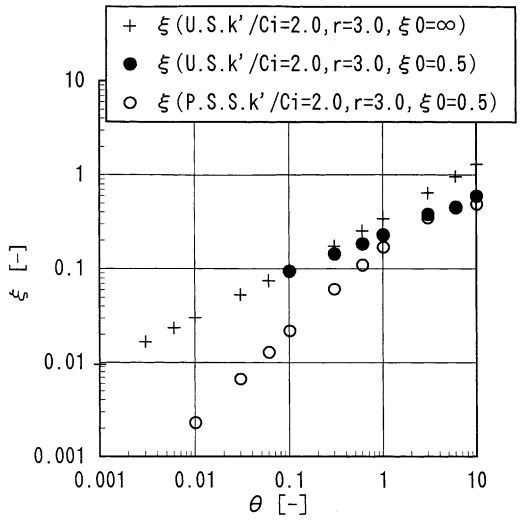

Fig. 12. Comparison between PSS and US for upper limit $\xi_0 = 0.5$ (case 1 and $m = 1$).

If $k_1 \ll k_2$, the rate-determining step is the first step in Eq. (39) or Eq. (40), and the rate of polymerization to the solid (elastic rubber) is assumed to be proportional to the water content or the first-order of water concentration.

The diffusion coefficient of water in the uncured zone (viscous fluid) seems to be slightly larger than that in the cured zone (elastic rubber), i.e., $r \geq 1$, and C_{2x} also seems to be slightly larger than C_{1x} in the cured zone (elastic rubber), i.e., $m \geq 1$.

Hitherto models were calculated under the condition of $C_2 = 0$ at $x_2 = \infty$. Usually, x_2 is limited and assumed to be L. Under these conditions, the results of the numerical calculation (Appendix B) with Eqs. (B.2), (B.3) and (B.8)–(B.10) are shown in Fig. 12, where the upper limit ξ_0 is 0.5. When θ is greaterthan 1, the PSS and US models with the upper limit are also in good agreement. Of course, as ξ approaches the upper limit ξ_0, or more than ξ_0, the results of the US model in the semi-infinite condition and those of the US and PSS models in the finite condition diverge.

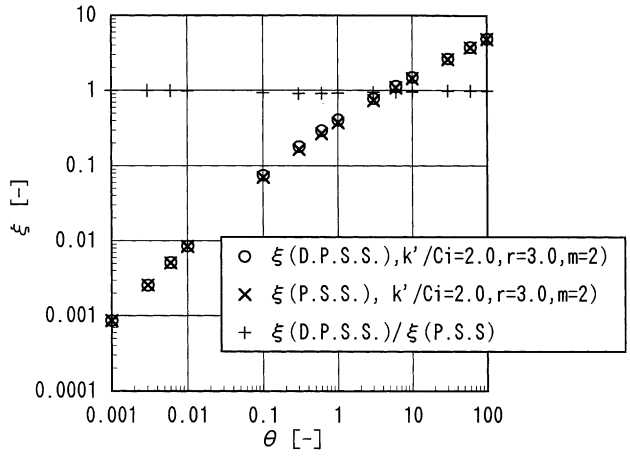

Fig. 13. Comparison between PSS with and without Danckwerts' condition ($k'/C_i = 2$, $r = 3$, $m = 2$ and case 1).

The experimental results and the PSS model results were compared. The experimental and the PSS model results coincided experimentally and theoretically. The PSS models of case 1 with and without Danckwerts' condition equation (23) were solved (Appendix C). The two results are the same, as shown in Fig. 13. ξ (DPSS) and ξ (PSS) mean ξ of PSS with and without Dackwerts' condition. Thus, it is unnecessary to consider the PSS model with Danckwerts' condition equation (23).

This paper studied the kinetics of the one-part curing system. However, the kinetics of these phenomena of the slow oxidation reaction of metals in air or the degradation of a polymer by oxygen and UV or γ-radiation can be similarly analyzed from this method.

7. Conclusions

The curing speed of a moisture-curable one-part sealant is attributed to the moving boundary problems of mass transfer and the reaction. PSS and US models were studied. These models were expressed by dimensionless equations ξ and θ with only three dimensionless parameters: r, k'/C_i and m. The PSS models, which are easy to calculate, and US models with two boundary conditions and $m = 1$ and $m \neq 1$ were compared. All four cases had similar results. When θ is greater than 1, the PSS and US results were in good agreement. The influence of the parameters were evaluated. The effect of k'/C_i on the curing speed was very significant, but the effects of m and r were small. Values of m and r of less than 1 had a slightly greater effect than those greater than 1. These results show that the rate-determining step of the curing speed depends on the cured zone's condition but does not depend on the uncured zone's condition. The moisture-curable one-part sealant usually cures at $\theta = kT$, which is grater than 1 because k is greater than 1.0 per day and T is greater than 1 day. Two boundary conditions were studied. Case 2 was more accurate than case 1 on the basis of theoretical and physical phenomena. The curing speed in case 2 was slightly slower than in case 1. However, the results for both conditions were almost the same, especially when θ was greater than 1. Thus, case 1 is accurate enough to study this phenomena. In designing these sealants, we can calculate or use the PSS model of case 1 with sufficient accuracy. The PSS model with the finite distance condition also agreed with the US model with the finite distance condition, when θ was greater than 1. The numerical method by Murray was applied to this one-part curing system and its results coincided with those by our US model. Thus, US models are adequate mathematically.

We studied the slow reaction system with moving boundary conditions mathematically and experimentally. Exact solutions (US models) suggested that even the slow reaction system with moving boundary conditions can be approximated by simple PSS solutions (PSS models) in the limited condition where θ is greater than 1. Experimental results supported these models.

These presented models can also be applied to the kinetics of similar phenomena such as slow oxidation reactions of metals in air or the degradation of a polymer by oxygen and UV or γ-radiation.

Acknowledgements

The author would like to thank Prof. Kenji Hashimoto (Fukui University of Technology) for discussions on this research work.

Appendix A. Boundary condition for case 2

Eq. (A.1) is obtained from the definition of N_2:

$$\frac{\partial N_2}{\partial x_2} = -D_2 \frac{\partial^2 C_2}{\partial x_2^2} \tag{A.1}$$

From Eq. (A.1), Eq. (A.2) is given in the uncured zone:

$$\frac{\partial C_2}{\partial t} = D_2 \frac{\partial^2 C_2}{\partial x_2^2} - kC_2 = -\frac{\partial N_2}{\partial x_2} - R_c \tag{A.2}$$

Eq. (A.2) is integrated from 0 to the curing time T:

$$\int_0^T \left.\frac{\partial C_2}{\partial t}\right|_{x_2=X} \mathrm{d}t = -\int_0^T \left.\frac{\partial N_2}{\partial x_2}\right|_{x_2=X} \mathrm{d}t - \int_0^T R_c|_{x_2=X}\,\mathrm{d}t \tag{A.3}$$

$$\int_0^T \left.\frac{\partial C_2}{\partial t}\right|_{x_2=X} \mathrm{d}t = C_{2x} - 0 = C_x \tag{A.4}$$

$$\int_0^T R_c|_{x_2=X}\,\mathrm{d}t = k' \tag{A.5}$$

We postulate that, after the total flux from $t = 0$ to T at any uncured face has reached the specified value, its face changes from the uncured region to the cured region and its specified value is constant wherever this face is located. Eq. (A.6) is expressed from this definition:

$$Q(T(X)) = \int_0^T N_2|_{x_2=X}\,\mathrm{d}t \tag{A.6}$$

$Q(T(X))$ is differentiated by X and its derivative is zero from the definition of $Q(X(T))$:

$$\frac{\mathrm{d}Q}{\mathrm{d}X} = \frac{\partial Q}{\partial T}\frac{\mathrm{d}T}{\mathrm{d}X} + \frac{\partial Q}{\partial X} = N_2|_{x_2=X}\frac{\mathrm{d}T}{\mathrm{d}X} + \int_0^T \left.\frac{\partial N_2}{\partial x_2}\right|_{x_2=X} \mathrm{d}t = 0,$$

$$\int_0^T \left.\frac{\partial N_2}{\partial x_2}\right|_{x_2=X} \mathrm{d}t = -N_2(X)\frac{\mathrm{d}T}{\mathrm{d}X} \tag{A.7}$$

From Eqs. (A.3)–(A.5) and (A.7), Eq. (10) is expressed.

Appendix B. Finite distance condition

First, we consider PSS models of not semi-infinite but finite distance L.

From Eq. (2) and the following B.C., Eq. (B.1) is obtained:

At B.C. $x = 0$, $C_2 = C_x$ and $x = L$, $\mathrm{d}C_2/\mathrm{d}x = 0$,

$$N = -D_2 \left.\left(\frac{\mathrm{d}C_2}{\mathrm{d}x}\right)\right|_{x=0} \beta\sqrt{kD_2}C_{2x} \tag{B.1}$$

Here, β is defined by Eq. (B.2):

$$\beta = \frac{\exp\{(L-X)\sqrt{k/D_2}\} - \exp\{-(L-X)\sqrt{k/D_2}\}}{\exp\{(L-x)\sqrt{k/D_2}\} + \exp\{-(L-X)\sqrt{k/D_2}\}} = \frac{1-\exp\{-(4/\sqrt{r})(\xi_0-\xi)\}}{1+\exp\{-(4/\sqrt{r})(\xi_0-\xi)\}} \tag{B.2}$$

The dimensionless PSS equation in the finite condition of case 1 is expressed by Eq. (B.3):

$$\frac{\mathrm{d}\xi}{\mathrm{d}\theta} = \frac{1}{2(k'/C_i)\{2\xi + (1/\beta\sqrt{r})\}} \tag{B.3}$$

B.C. $\theta = 0, \xi = 0$

If $\beta = 1$, Eq. (B.3) coincides with Eq. (9) by integration.

Next, the US model of the finite condition L of case 1 is studied.

From Eq. (19) and B.C. of $x_2 = X$, $C_2(S) = C_x/S$ and $x_2 = L$, $\mathrm{d}C_2(S)/\mathrm{d}x_2 = 0$, Eq. (B.4) is given. C_x depends only on X and T and does not depend on t. Thus, the Laplace transformation of t on C_x is C_x/S.

$$C_2(S) = \left(\frac{C_x}{S}\right)\left[\frac{\exp\{-\sqrt{(S+k)/D_2}(x_2-X)\}}{1+\exp\{-2\sqrt{(S+k)/D_2}(L-X)\}} + \frac{\exp\{\sqrt{(S+k)/D_2}(x_2-X)\}}{1+\exp\{2\sqrt{(S+k)/D_2}(L-X)\}}\right] \tag{B.4}$$

Eq. (B.4) is differentiated by x_2 and $x_2 = X$ is introduced.

$$\left.\frac{\mathrm{d}C_2(S)}{\mathrm{d}x_2}\right|_{x_2=X} = \left(-\frac{C_x}{S}\right) \times \left\{\frac{\sqrt{(S+k)/D_2}}{1+\exp(-2\sqrt{(S+k)/D_2}(L-X))} - \frac{\sqrt{(S+k)/D_2}}{1+\exp(2\sqrt{(S+k)/D_2}(L-X))}\right\} \tag{B.5}$$

Eq. (B.5) is expanded by the Taylor's series:

$$\left.\frac{dC_2(S)}{dx_2}\right|_{x_2=X} = \frac{C_x}{S}\sqrt{\frac{S+k}{D_2}}\left\{\sum_{n=0}^{\infty}\left((-1)^n \exp\left(-2n\sqrt{\frac{S+k}{D_2}}(L-X)\right)\right) -(-1)^n \exp\left(-2(n+1)\sqrt{\frac{S+k}{D_2}}(L-X)\right)\right\} \quad (B.6)$$

$$N_{2x}(S) = -D_2\left.\frac{dC_2(S)}{dx_2}\right|_{x_2=X} = -\frac{\sqrt{D_2}}{S}C_x\sqrt{S+k} + 2\sqrt{D_2}C_x\frac{\sqrt{S+k}}{S}\sum_{n=1}^{\infty}(-1)^n \times\exp\left(\frac{-2n(L-X)}{\sqrt{D_2}}\sqrt{S+k}\right)$$

The inverse Laplace transformation of the above equation is expressed by Eq. (B.7):

$$N_2(x=X) = C_x\sqrt{D_2k}\left\{\operatorname{erf}\sqrt{\theta} + \left(\frac{1}{\sqrt{\pi\theta}}\right)\exp(-\theta)\right\} +C_x\sqrt{D_2k}\sum_{n=1}^{\infty}(-1)^n\left\{2\frac{1}{(\pi\theta)^{1/2}} \times\exp\left(-\frac{4n^2\eta^2}{r\theta}\right) + \exp\left(-\frac{4n\eta}{\sqrt{r}+\theta}\right) \times\operatorname{erfc}\left(\frac{2n\eta}{\sqrt{r\theta}} - \sqrt{\theta}\right) - \exp\left(\frac{4n\eta}{\sqrt{r}+\theta}\right) \times \operatorname{erfc}\left(\frac{2n\eta}{\sqrt{r\theta}} + \sqrt{\theta}\right)\right\} \quad (B.7)$$

In Eq. (B.7), η is defined by $((\mathrm{L}-\mathrm{X})/2)\sqrt{\mathrm{k}/0_1}$.

From Eqs. (5a), (26) and (B.7), first C_x/C_i is obtained and the dimensionless equation of $d\eta/d\theta$ is expressed by Eqs. (B.8)–(B.10):

$$\frac{d\eta}{d\theta} = -\frac{(1-C_x/C_i)\exp\{-(\xi_0-\eta)^2/\theta\}}{2(k'/C_i)\sqrt{\pi\theta}\operatorname{erf}(\xi_0-\eta)/\sqrt{\theta}} \quad (B.8)$$

$$\frac{C_x}{C_i} = \frac{\exp(-(\xi_0-\eta)^2/\theta)}{\exp\{-(\xi_0-\eta)^2/\theta\} + \sqrt{r}\{(\operatorname{erf}\sqrt{\theta})\sqrt{\pi\theta} + \exp(-\theta)\}} \times\operatorname{erf}(\theta\{(\xi_0-\eta)/\sqrt{\theta}\} + R \quad (B.9)$$

$$R = \sqrt{r}\exp(-\theta)\sum_{n=1}^{\infty}(-1)^n\left\{2\exp\left(-\frac{4n^2\eta}{r\theta}\right)\operatorname{erf}\left(\frac{\xi_0-\eta}{\sqrt{\theta}}\right) +\sqrt{\pi\theta}\operatorname{erf}\left(\frac{\xi_0-\eta}{\sqrt{\theta}}\right)\exp\left(-\frac{4n\eta}{\sqrt{r}}+\theta\right) \times\operatorname{erfc}\left(\frac{2n\eta}{\sqrt{r\theta}} - \sqrt{\theta}\right) - \exp\left(-\frac{4n\eta}{\sqrt{r}}+\theta\right) \times \operatorname{erfc}\left(\frac{2n\eta}{\sqrt{r\theta}} + \sqrt{\theta}\right)\right\} \quad (B.10)$$

Appendix C. PSS models with Danckwerts' conditions

From Eqs. (3) and (5), Eq. (C.1) is obtained:

$$\frac{dX}{dT} = \left(\frac{\sqrt{kD_2}}{k'}\right)C_{2x} \quad (C.1)$$

Dimensionless equation (C.1) is given by Eq. (C.2):

$$\frac{d\xi}{d\theta} = \left(\frac{\sqrt{r}}{2}\right)\left(\frac{C_{2x}}{k'}\right) \quad (C.2)$$

From Eqs. (1), (3), (23) and (C.1), Eq. (C.3) is obtained:

$$\sqrt{kD_2}\left(\frac{1}{m}-1\right)\left(\frac{C_{2x}}{k'}\right)^2 + \left(\frac{D_1}{mX}+\sqrt{kD_2}\right)\left(\frac{C_{2x}}{k'}\right) -\left(\frac{D_1}{X}\right)\left(\frac{C_i}{k'}\right) = 0 \quad (C.3)$$

From Eq. (C.3), (C_{2x}/k') is calculated and its value is introduced in Eq. (C.2). Eq. (C.2) is the curing speed of the PSS model with Danckwerts' condition.

References

[1] J.R. Panek, J.P. Cook, Construction Sealants and Adhesives, Wiley, New York, 1991.
[2] C.Y. Wen, Noncatalytic solid reactions models, Ind. Eng. Chem. 60 (9) (1968) 34–54.
[3] M. Ishida, K. Yoshino, T. Shirai, The applicability of the pseudo-steady-state approximation to moving boundary problems for spheres, J. Chem. Eng. Jpn. 3 (1) (1970) 49–54.
[4] K. Yoshida, D. Kunni, Application of collocation technique for moving boundary problems in solid–gas reactions, J. Chem. Eng. Jpn. 8 (5) (1975) 417–419.
[5] W.D. Murray, F. Landis, Numerical and machine solutions of transient heat-conduction problems involving melting or freezing: Part I, J. Heat Transfer ASME Trans. 81C (1959) 106–112.
[6] H.S. Carslow, J.C. Jaeger, Conduction of Heat in Solids, Clarendon Press, Oxford, 1973, pp. 134–135.
[7] J. Crank, The Mathematics of Diffusion, Oxford University Press, Oxford, 1995, pp. 286–337.
[8] P.V. Danckwerts, Trans. Faraday Soc. 46 (1950) 701–712.
[9] T. Matsui, H. Kojima, M. Yabu, The analysis of curing kinetics of sealants, J. Soc. Chem. Eng. Jpn. 25 (1) (1999) 117–123.